Probing the quantum ground state of a spin-1 Bose-Einstein condensate with cavity transmission spectra

J. M. Zhang,[1,2] S. Cui,[2] H. Jing,[2] D. L. Zhou,[1] and W. M. Liu[1]
[1]*Beijing National Laboratory for Condensed Matter Physics, Institute of Physics, Chinese Academy of Sciences, Beijing 100080, China*
[2]*Department of Physics, Henan Normal University, Xinxiang 453007, China*
(Received 9 July 2009; published 26 October 2009)

We propose to probe the quantum ground state of a spin-1 Bose-Einstein condensate with the transmission spectra of an optical cavity. By choosing a circularly polarized cavity mode with an appropriate frequency, we can realize coupling between the cavity mode and the magnetization of the condensate. The cavity transmission spectra then contain information of the magnetization statistics of the condensate and thus can be used to distinguish the ferromagnetic and antiferromagnetic quantum ground states. This technique may also be useful for continuous observation of the spin dynamics of a spinor Bose-Einstein condensate.

DOI: 10.1103/PhysRevA.80.043623 PACS number(s): 03.75.Mn, 32.10.Dk, 37.10.Vz, 42.50.Pq

Spinor Bose-Einstein condensates (BECs) distinguish themselves from their scalar counterparts by their much richer internal structures and dynamics [1,2]. Based on the single mode approximation (SMA) which is valid in most cases, the quantum eigenstates of a spinor BEC have been extensively and thoroughly studied with sophisticated algebraic techniques [3–5]. Especially, for the spin-1 case which we focus on in this paper, it is found that there are two possibilities for the ground state. Depending on a single parameter, the ground state can be either of an antiferromagnetic (AFM) or a ferromagnetic (FM) nature. The two phases differ in their rotational properties: the AFM ground state is a SU(2) singlet and thus isotropic [6], while the FM ground state is a SU(2) multiplet heavily degenerate and thus can be well directed [up to the uncertainty principle associated with the SU(2) algebra]. From the point of view of quantum phase transition, these two phases deserve to be distinguished experimentally for their own sake [7].

In this paper we propose a method based on cavity quantum electrodynamics techniques to fulfill this object. The basic idea is similar to that of Mekhov *et al.* in Ref. [8], where they proposed to probe the superfluidity–Mott-insulator transition of cold atoms in optical lattices with cavity transmission spectra. In the dispersive regime, atoms inside the cavity shift the cavity frequency and in turn influence the cavity transmission spectra. The superfluidity and Mott-insulator phases differ in their atom number statistics and thus lead to drastically different cavity transmission spectra, which can be used inversely to differentiate the two phases. In their proposal, it is adequate to treat the atoms in a two-level fashion with the atomic levels structureless. However, here in our case, we have to go beyond the two-level model and take into account the detailed and realistic atomic level structure. In this way, we can retrieve the vector polarizability [9] of the atom that is dropped artificially in the two-level model. It follows that by choosing a circularly polarized cavity mode, the cavity photon couples not only to the total atom number but also to the total magnetization. The latter effect allows us to do our job since the cavity transmission spectra carry information of the magnetization statistics of the BEC, which are absolutely different in the two phases.

We assume that a spin-1 BEC of N alkali atoms of a certain type is loaded inside an optical cavity [10]. This system is probed with a σ_+ polarized laser so that the relevant cavity mode coupled with the atoms is also σ_+ polarized. The bare frequency ω_c of this cavity mode is chosen to resolve the alkali D line (fine structure) and placed relatively near the D_1 transition [11]. However, the detuning between the D_1 transition and the cavity mode frequency is still large enough not to resolve the hyperfine structures of the D_1 line. More precisely, we have $\Delta_{HFS1} \ll |\omega_c - \omega_{D_1}| \ll |\omega_c - \omega_{D_2}|$, where Δ_{HFS1} is the magnitude of the hyperfine splitting of the D_1 line and ω_{D_1} and ω_{D_2} are the average frequencies of the hyperfine levels of D_1 and D_2, respectively. In the Appendix we show that the effective Hamiltonian describing the atom-cavity photon interaction is ($\hbar=1$ throughout in this paper)

$$H_{int} = \sum_m \left(1 + \frac{m}{2}\right) U_0 \int dx u^2(x) \psi_m^\dagger(x) \psi_m(x) a^\dagger a. \qquad (1)$$

Here $\psi_m(x)$ $(m=0, \pm 1)$ is the field annihilation operator for an atom in the hyperfine state $|F=1, m\rangle$ at position x (the quantization direction is along the cavity axis and is denoted as z direction) and a is the annihilation operator for the cavity photon. The cavity mode function with its maximum normalized to unity is denoted as $u(x)$. The parameter U_0 characterizes the strength of the ac-Stark shifts of the atomic levels per photon in the viewpoint of the atoms or, alternatively, the magnitude of the cavity frequency shift per atom in the viewpoint of the photons. Formally, we can write U_0 as $U_0 = g_0^2/(\omega_c - \omega_{D_1})$ by introducing an effective atom-photon coupling strength g_0, which incorporates the overall effect of coupling with all the hyperfine levels in the D_1 line.

Here some comments are in order. The main feature of Hamiltonian (1) is the spin dependence of the level shifts, which can be interpreted in terms of a fictitious magnetic field. In most experiments aiming to study intrinsic spin dynamics of a spinor BEC, this effect is (and should be) avoided or minimized by taking the laser beam to be linearly polarized or with a detuning too large to resolve the D line or both (an exception being Ref. [12]). However, for the purpose of continuous observation of spin dynamics and spin magnetization, this effect proves to be useful. Actually, it is exactly the same physics that underlies the Faraday rotation

spectroscopy developed recently for *in situ* observation of a spinor BEC [13–15]. Because the cavity mode is σ_- polarized, the plus sign in front of $\frac{m}{2}$ in Eq. (1) should be replaced with a minus sign. That is, the σ_+ and σ_- polarized lights respond differently to a given atomic sample—the essence of the Faraday rotation effect.

For the spinor BEC, we assume that the SMA is valid and rewrite the atomic field operators as $\psi_m(x)=\phi(x)c_m$. Here $\phi(x)$ denotes the common spatial mode (normalized to unity) for the three spin components and c_m is the annihilation operator associated with the corresponding spin component. Under the SMA, we can rewrite Hamiltonian (1) as

$$H_{int} = U\left(\hat{N} + \tfrac{1}{2}\hat{M}\right)a^\dagger a, \tag{2}$$

where $\hat{N}=\Sigma_m c_m^\dagger c_m$ is the total atom number and $\hat{M}=\Sigma_m m c_m^\dagger c_m$ is the total magnetization. The parameter $U \equiv U_0\int dx u^2(x)\phi^2(x)$ is proportional to the overlap between the cavity mode function and the condensate mode function. In general, the extension of a condensate is much larger than the period of $u^2(x)$ in the axial direction while much smaller than its waist in the transverse direction. Therefore, for a condensate placed around the axis of the cavity, the integral can be well approximated with 1/2, i.e., $U \simeq U_0/2$. We note that $\hat{N}$ and $\hat{M}$ commute with both H_{int} and the Hamiltonian of the spinor BEC itself. Therefore, we have a quantum nondemolition measurement.

Assume the probe laser is of frequency ω_p. The Heisenberg equation (in the frame rotating at ω_p) for the cavity mode annihilation operator is

$$\dot{a} = -i\left[\omega_c - \omega_p + U\left(\hat{N} + \tfrac{1}{2}\hat{M}\right)\right]a - \kappa a + \eta, \tag{3}$$

where κ is the damping rate of the cavity mode and η is the driving amplitude. The damping term leads to the stationary solutions of a and the photon number [8],

$$a_{st} = \frac{\eta}{\kappa + i(\Delta + U\hat{M}/2)}, \tag{4a}$$

$$\hat{n}_{st} = a_{st}^\dagger a_{st} = \frac{\eta^2}{\kappa^2 + (\Delta + U\hat{M}/2)^2}, \tag{4b}$$

where $\Delta=\omega_c+UN-\omega_p$ is the shifted cavity-probe detuning. The expectation value of $\hat{n}_{st}$ over a prescribed state of the spinor BEC is then

$$n_{st} = \langle \hat{n}_{st} \rangle = \sum_{M=-N}^{N} f_M \frac{\eta^2}{\kappa^2 + (\Delta + UM/2)^2}, \tag{5}$$

where f_M is the probability for $\hat{M}$ taking value M in the prescribed state. We have $\Sigma_M f_M=1$, where the sum is over all the possible values of M. As pointed out in Ref. [16], the total photon number contains incoherent contributions of a series of coherent states, the Mth of which is of amplitude $\eta/[\kappa+i(\Delta+UM/2)]$ and of weight f_M. Mathematically, we see from Eq. (5) that n_{st}, as a function of the detuning Δ, is a weighted sum of a series of Lorentz functions, which are evenly displaced with $U/2$ and of full width at half maximum 2κ. The point is that the cavity transmission spectra (proportional to n_{st}) contain information of the atomic statistics embodied in f_M.

We now apply the formalism developed above to the two possible phases of a spin-1 BEC. For a spin-1 BEC in the SMA, the Hamiltonian accounting for the spin dynamics is $H_s=W\mathbf{S}^2$ [3], with the spin operator $\mathbf{S}\equiv(S_x,S_y,S_z)=c_m^\dagger(S_x^{mn},S_y^{mn},S_z^{mn})c_n$. The parameter W is proportional to the difference of s-wave scattering lengths in the two total spin channels. Obviously, the sign of W determines the nature of the ground state. If $W>0$, the ground state is of total spin $S=0$ and given explicitly as [4–6]

$$|G\rangle_{\mathrm{AFM}} = |S=0,M=0\rangle \propto (A^\dagger)^{N/2}|0\rangle, \tag{6}$$

where the scalar (rotationally invariant) operator $A^\dagger \equiv c_0^{\dagger 2} - 2c_{+1}^\dagger c_{-1}^\dagger$. This state is a singlet and also the unique ground state. For this AFM ground state, the magnetization has no fluctuations at all. The only nonvanishing term in Eq. (5) is $M=0$. Therefore, by scanning the probe frequency ω_p, we get the intracavity photon number as a single Lorentz function,

$$n_{st}(\Delta) = \frac{\eta^2}{\kappa^2 + \Delta^2}, \tag{7}$$

with a width of 2κ and maximum height of unity (in units of η^2/κ^2, the maximum possible intracavity photon number). Note that it is of the same shape as that of a bare cavity though the center is shifted by UN.

If $W<0$, the ground state is of total spin $S=N$ and thus $2N+1$-fold degenerate. Explicitly, we have as a set of orthonormal basis [4,5],

$$|G\rangle_{\mathrm{FM}} = |S=N,M\rangle \propto (S_-)^{N-M}(c_{+1}^\dagger)^N|0\rangle, \tag{8}$$

where $S_-=\sqrt{2}(c_0^\dagger c_{+1}+c_{-1}^\dagger c_0)$ is the lowering operator for S_z. These $2N+1$ states each has a definite magnetization; thus the corresponding transmission spectrum is also a single Lorentz function (but the center of which may vary). However, here we are most interested in the experimentally most accessible states—angular momentum coherent states—states that can be obtained by rotating the z-aligned state $|N,N\rangle$,

$$e^{-i\theta\vec{\zeta}\cdot\vec{S}}|N,N\rangle = \frac{(x_{+1}c_{+1}^\dagger + x_0 c_0^\dagger + x_{-1}c_{-1}^\dagger)^N}{\sqrt{N!}}|0\rangle. \tag{9}$$

Here $\vec{\zeta}=(-\sin\phi,\cos\phi,0)$ perpendicular to the z axis is the axis of rotation, while θ is the angle of rotation or inclination angle. The x_i's are determined by $e^{-i\theta\vec{\zeta}\cdot\vec{S}}c_{+1}^\dagger e^{i\theta\vec{\zeta}\cdot\vec{S}}=x_{+1}c_{+1}^\dagger + x_0 c_0^\dagger + x_{-1}c_{-1}^\dagger$. The state constructed in Eq. (9) breaks the symmetry of H_s and defines a direction (θ,ϕ) in that it is the eigenstate of $S_{n(\theta,\phi)}=\sin\theta\cos\phi S_x+\sin\theta\sin\phi S_y+\cos\theta S_z$ with eigenvalue N. These states can be readily prepared with a proper radio-frequency (rf) pulse from the state $|N,N\rangle$ [17]. For such a state, the weight coefficients of the Fock states $|N_{+1},N_0,N_{-1}\rangle$ follow the triple-nominal distribution,

$$P(N_{+1},N_0,N_{-1}) = \frac{N!}{N_{+1}!\,N_0!\,N_{-1}!} p_{+1}^{N_{+1}} p_0^{N_0} p_{-1}^{N_{-1}}, \quad (10)$$

with $p_i=|x_i|^2$ and $\Sigma_i p_i=1$. Explicitly, we have $(p_{+1},p_0,p_{-1}) = (\cos^4\frac{\theta}{2}, 2\cos^2\frac{\theta}{2}\sin^2\frac{\theta}{2}, \sin^4\frac{\theta}{2})$. Note that p_i is independent of the azimuth angle ϕ. This is reasonable since all angular momentum coherent states with the same inclination angle θ are connected by rotations around the z axis. Therefore they share the same distribution $P(N_{+1},N_0,N_{-1})$.

The probability distribution function f_M can be generated in a random-walk process. Image a particle, initially at the origin, performing random walks on the real axis. At each step, the particle either moves rightward or leftward or just keeps still, with probabilities p_{+1}, p_{-1}, and p_0, respectively. Then f_M is just the probability of arriving at M after N steps. In other words, M is the sum of N independent random variables $\{X_k, 1\le k\le N\}$, the common distribution function of which is $Pr(X_k=i)=p_i$, with $i=0,\pm 1$. This interpretation enables us to calculate f_M both analytically and numerically. Analytically, for $N\gg 1$, by the central limit theorem, we can approximate f_M with the normal distribution

$$f_M = \frac{1}{\sqrt{2\pi}\sigma}\exp\left(-\frac{(M-M_c)^2}{2\sigma^2}\right), \quad (11)$$

where $M_c=N\cos\theta$ and $\sigma=\sqrt{N}\sigma_0$ (here $\sigma_0=\sqrt{\frac{1}{2}\sin^2\theta}$ being the variance of X_k) are the average value and variance of M, respectively. Numerically, the characteristic function of f_M is $\chi(t)=(p_{+1}e^{+it}+p_0+p_{-1}e^{-it})^N$. By an inverse Fourier transform, we get f_M determined [it is just the coefficient of e^{iMt} in the expansion of $\chi(t)$]. The two approaches yield the same result up to a high precision. In Fig. 1(a), we show the distribution f_M for four different inclination angles with the total atom number $N=10^6$. We see that the larger the absolute value of $\sin\theta$, the larger the fluctuations of M. For all cases, we see a clear $\sqrt{N}$ scaling of σ.

We calculate the intracavity photon number n_{st} by approximating f_M with Eq. (11) and replacing the sum with an integral. The integral can be further understood as the convolution of the probability distribution function f_M and a Lorentz function. We can then use the convolution theorem to first solve the Fourier transforms of the two functions form their product and then take an inverse Fourier transform. We get

$$n_{st}(\Delta) = \frac{\eta^2}{2\kappa}\int_{-\infty}^{+\infty} dt e^{it(\Delta-\Delta_c)} \times e^{-\kappa|t|-t^2U^2\sigma^2/8}, \quad (12)$$

where $\Delta_c=-M_cU/2$. Obviously, the procedure can be done inversely, i.e., from the cavity transmission spectra observed experimentally, we can infer the distribution of the magnetization by Fourier transforms.

We can read two facts from Eq. (12). First, the shape of n_{st} as a function of Δ is shifted by Δ_c from that depicted in Eq. (7). This overall shift is due to the average deviation of M from zero and thus has a classical nature. Second, the shape of n_{st} is broadened compared to that in Eq. (7), which is due to the fluctuations of M around the mean and thus has a quantum nature. The shift and broadening are appreciable if $(M_cU,\sigma U)\gg\kappa$ or, in terms of N, $(NU,\sqrt{N}U)\gg\kappa$. Currently, g_0 is about $2\pi\times 15$ MHz and the linewidth κ of the cavity can be made as small as $2\pi\times 1.0$ MHz [18–20]. By taking the detuning $\Delta_{ca}=\omega_c-\omega_{D_1}$ to $2\pi\times 40$ GHz, we get $U\sim 2\pi\times 2.8$ kHz. The atom number of a spinor BEC is typically on the order of 10^6. Thus we see the first condition $NU\gg\kappa$ is well satisfied while the second condition $\sqrt{N}U\gg\kappa$ is marginally satisfied. In the near future, we expect κ can be reduced by one order and then the second condition can be well met also.

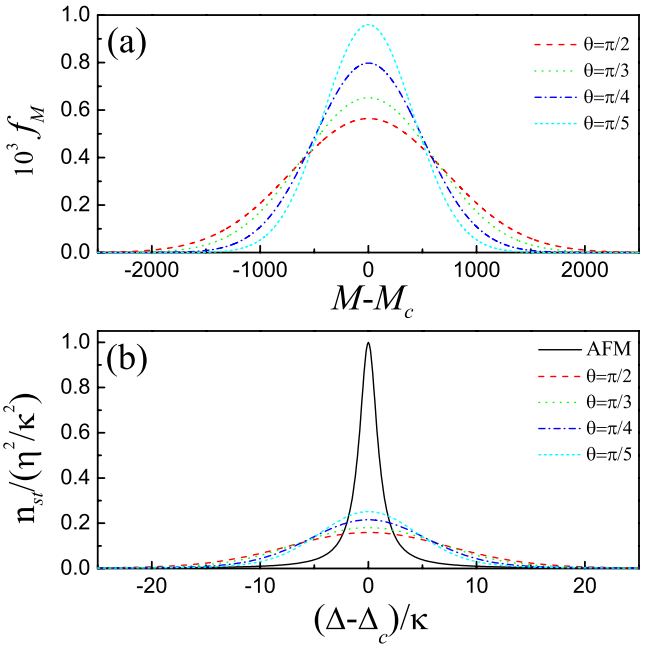

FIG. 1. (Color online) (a) Probability distribution function f_M of the magnetization M of FM ground states with different inclination angles. (b) Intracavity photon number at steady state n_{st} as a function of the detuning Δ. The solid line corresponds to the AFM ground state. Other lines correspond to FM ground states in (a). The parameters are $N=10^6$ and $U=0.01\kappa$. For the horizontal labels, $M_c=N\cos\theta$ and $\Delta_c=-M_cU/2$ in the FM case, while $M_c=0$ and $\Delta_c=0$ in the AFM case.

In Fig. 1(b), we present the intracavity photon number at steady state n_{st} as a function of the detuning Δ. For the AFM ground state, the curve (solid line) is a simple Lorentzian centered at $\Delta_c=0$ and with width 2κ. This is the only possibility. However, for the FM ground states, depending on the inclination angle θ, the center and width of the curve vary widely (the figure may be a bit misleading, but note that we have artificially shifted the curves to a common center; see the labels of the horizontal axes). Especially, the broadening effect is apparent compared to the AFM case (here we have $\sqrt{N}U/\kappa=10$). Thus the AFM and FM ground states can be distinguished on one hand by the different shapes of the corresponding spectra [21] and on the other hand by their responses to rf pulses (or a transverse magnetic field). Under the action of rf pulses, the AFM ground state remains unaltered since it is rotationally invariant, so the cavity transmission spectra are unchanged. In contrast, a FM ground state can be tickled to other directions and thus both the center and the width of the transmission spectra will change.

An alternative and more convenient method may be just

reversing the polarization of the probe laser. Because the σ_+ and σ_- polarized cavity modes couple to $\hat{M}$ and $-\hat{M}$, respectively, it is easy to see that for the AFM case, the transmission spectra are unaffected, while for the FM case, the transmission spectra are reflected to be centered at $-\Delta_c$. The distance between the two centers is on the order of NU, which is much larger than κ; therefore this effect can be readily observed. This method makes evident the similarity between our approach and the Faraday rotation spectroscopy.

In summary, we have shown that by choosing a circularly polarized cavity mode, we can achieve coupling between the photon number with the magnetization, i.e., the z component of the total spin of the spinor BEC. Full statistics of the magnetization of the spinor BEC can be extracted from the cavity transmission spectra and this allows us to discern the AFM and FM phases, which, due to their different rotational properties, possess absolutely different magnetization statistics. Our discussion has been focused on the thermodynamical properties of the BEC (ground state oriented). However, it is clear that the technique can also be used for observing real-time evolution of a spinor BEC. Moreover, since the condition $NU \gg \kappa$ can be readily fulfilled, the sensitivity can be high.

It should be emphasized that our discussion has been greatly simplified by neglecting the center-of-mass motion of the BEC and by the SMA [without the two approximations, we cannot reduce Eq. (1) to Eq. (2)]. These approximations are reasonable if the probe is weak enough. For future works, however, the strong probe case is worth investigation. If the probe is so strong that the intracavity optical lattice cannot be neglected, center-of-mass motion of the spinor BEC can be excited. Moreover, since the optical lattices felt by different spin components are different, a dynamical SMA is inappropriate. The situation is further complicated by the back action of the BEC on the cavity mode. In the end, this system may exhibit many interesting nonlinear effects [22].

This work was supported by NSF of China under Grants No. 10874235, No. 60978019, No. 10775176, No. 10934010, and No. 10975181 and NKBRSF of China under Grants No. 2009CB930704, No. 2006CB921400, No. 2006CB921206, and No. 2010CB922904. J.M.Z. would like to thank J. Ye for stimulating discussions.

APPENDIX: EFFECTIVE HAMILTONIAN

In this appendix we review the derivation of the effective Hamiltonian (1). The main concern is to demonstrate the Zeeman-like effect. General theory about this effect has actually been well established [23–25]. We include the derivation here just to serve our concrete purpose. For simplicity, we take the optical field to be classical; generalization to the quantum case is straightforward. The alkali atom in question is assumed to be in the $n^2S_{1/2}$ $F=1$ hyperfine ground state manifold. A laser with electric field $\vec{E}(t)=\vec{E}\exp(-i\omega_f t)+\text{c.c.}$ couples the atom to the $n^2P_{1/2}$ excited state manifold (D_1 line). Here it is assumed that the frequency of the laser is chosen so that the fine structure of the alkali D line is well resolved while the hyperfine structure is not. This is feasible since the fine structure splitting is generally three or four orders larger in magnitude than the hyperfine structure splitting for the alkali D line. For instance, the fine splitting of the D line of ^{87}Rb is $2\pi\times 7200$ GHz, while the hyperfine splitting of the D_1 line is $2\pi\times 814.5$ MHz.

We aim to derive an effective Hamiltonian confined in the $F=1$ ground state subspace. By second-order perturbation theory and taking the rotating wave approximation, we have [26]

$$H_{\text{eff}}=\frac{P_{g;F=1}(\vec{E}^*\cdot\vec{d})P_{D_1}(\vec{d}\cdot\vec{E})P_{g;F=1}}{\omega_f-\omega_{D_1}}, \tag{A1}$$

where $\vec{d}$ is the electric dipole operator and $P_{g;F=1}$ and P_{D_1} are the projection operators on the $F=1$ hyperfine ground state manifold and D_1 fine excited state manifold, respectively. That is, $P_{g;F=1}=\Sigma_m|n^2S_{1/2};F=1,m\rangle\langle n^2S_{1/2};F=1,m|$ and $P_{D_1}=\Sigma_{F,m}|n^2P_{1/2};F,m\rangle\langle n^2P_{1/2};F,m|$, where the sum is over all the possible values of F and m. For the latter, we can also transfer from the coupled representation to the uncoupled representation, i.e., equivalently we have

$$P_{D_1}=P_{e;J=1/2}\otimes P_I. \tag{A2}$$

Here $P_{e;J=1/2}$ is purely an electronic projection operator onto the $J=1/2$ excited state subspace, while P_I is purely a nuclear projection operator. We can also define the project operator

$$P_g=P_{g;J=1/2}\otimes P_I=P_{g;F=1}+P_{g;F=2}, \tag{A3}$$

which projects onto the ground state manifold up to the fine structure. Substituting Eqs. (A2) and (A3) into Eq. (A1) and noting that $P_gP_{g;F=1}=P_{g;F=1}$, we rewrite the effective Hamiltonian as

$$\begin{aligned}H_{\text{eff}}&=P_{g;F=1}\frac{P_g(\vec{E}^*\cdot\vec{d})P_{D_1}(\vec{d}\cdot\vec{E})P_g}{\omega_f-\omega_{D_1}}P_{g;F=1}\\&=P_{g;F=1}\left(\frac{P_{g;J=1/2}(\vec{E}^*\cdot\vec{d})P_{e;J=1/2}(\vec{d}\cdot\vec{E})P_{g;J=1/2}}{\omega_f-\omega_{D_1}}\right.\\&\quad\left.\otimes P_I\right)P_{g;F=1}.\end{aligned} \tag{A4}$$

Note that in the parentheses we have successfully separated the electronic part from the nuclear part. This is important since the external electric field couples with the electrons but not the nucleus. We define $\vec{D}=P_{e;J=1/2}\vec{d}P_{g;J=1/2}$, which is a vector operator (and so is $D^\dagger$). The electronic part in the parentheses in Eq. (A4) is then in the form $(\vec{E}^*\cdot\vec{D}^\dagger)(\vec{D}\cdot\vec{E})$, which can be rewritten in the form $D_i^\dagger D_jE_i^*E_j$, the scalar contraction of two rank-2 tensors, with the atomic and optical parts separated. We can decompose the dyadic $D_i^\dagger D_j$ into rank-0, 1, 2 irreducible tensors,

$$\begin{aligned}D_i^\dagger D_j&=\tfrac{1}{3}(\vec{D}^\dagger\cdot\vec{D})\delta_{ij}+\tfrac{1}{2}(D_i^\dagger D_j-D_j^\dagger D_i)\\&\quad+\left[\tfrac{1}{2}(D_i^\dagger D_j+D_j^\dagger D_i)-\tfrac{1}{3}(\vec{D}^\dagger\cdot\vec{D})\delta_{ij}\right],\end{aligned} \tag{A5}$$

with $E_i^*E_j$ done similarly. We note that since $D^\dagger D$ acts on a

two-dimensional Hilbert space, the rank-2 irreducible part vanishes identically. We can then contract the corresponding irreducible tensors to form scalars. The result is

$$\tfrac{1}{3}(\vec{D}^\dagger \cdot \vec{D})(\vec{E}^* \cdot \vec{E}) + \tfrac{1}{2}(\vec{D}^\dagger \times \vec{D}) \cdot (\vec{E}^* \times \vec{E}). \tag{A6}$$

Using the Wigner-Eckart theorem, we see that in the $J=1/2$ ground state subspace the scalar operator $\vec{D}^\dagger \cdot \vec{D}$ is proportional to the identity operator while the vector operator $\vec{D}^\dagger \times \vec{D}$ to $\vec{J}$. Thus the above equation is equivalent to

$$|\vec{E}|^2[\alpha - i\beta(\vec{e}^* \times \vec{e}) \cdot \vec{J}], \tag{A7}$$

with α and β being some constants and $\vec{e}=\vec{E}/|\vec{E}|$ being the laser polarization vector. Substituting this result into Eq. (A4) and using again the Wigner-Eckart theorem, we have finally

$$H_{\text{eff}} = \frac{|\vec{E}|^2}{\omega_f - \omega_{D_1}}[\alpha - i\gamma(\vec{e}^* \times \vec{e}) \cdot \vec{F}], \tag{A8}$$

with γ being some constant incorporating the Landé factor [27]. The first term describes a center-of-mass shift of the ground state multiplet, while the second term is in effect a Zeeman term—the very effect we are seeking. Note that for a linearly polarized laser the second term vanishes identically, while for σ_+ and σ_- polarized lasers, the fictitious magnetic fields point opposite.

Therefore we have shown how an effective Hamiltonian such as Eq. (1) can arise naturally under certain circumstances. To get the coefficients α and γ determined, it is better to resort to the dipole matrix elements tabulated in Ref. [28].

[1] D. M. Stamper-Kurn, M. R. Andrews, A. P. Chikkatur, S. Inouye, H.-J. Miesner, J. Stenger, and W. Ketterle, Phys. Rev. Lett. **80**, 2027 (1998).

[2] T. Ohmi and K. Machida, J. Phys. Soc. Jpn. **67**, 1822 (1998); T. L. Ho, Phys. Rev. Lett. **81**, 742 (1998).

[3] C. K. Law, H. Pu, and N. P. Bigelow, Phys. Rev. Lett. **81**, 5257 (1998).

[4] M. Koashi and M. Ueda, Phys. Rev. Lett. **84**, 1066 (2000).

[5] T. L. Ho and L. Yin, Phys. Rev. Lett. **84**, 2302 (2000).

[6] In this paper we assume that the total atom number N is even. For N being odd, the AFM ground state is of total spin $S=1$ and thus not strictly isotropic. However, that makes little difference or difficulty to our proposal; see discussions below.

[7] S. Ashhab and A. J. Leggett, Phys. Rev. A **65**, 023604 (2002).

[8] I. B. Mekhov, C. Maschler, and H. Ritsch, Nat. Phys. **3**, 319 (2007).

[9] K. D. Bonin and V. V. Kresin, *Electric-Dipole Polarizabilities of Atoms, Molecules, and Clusters* (World Scientific, Singapore, 1997).

[10] F. Brennecke, T. Donner, S. Ritter, T. Bourdel, M. Köhl, and T. Esslinger, Nature (London) **450**, 268 (2007); Y. Colombe, T. Steinmetz, G. Dubois, F. Linke, D. Hunger, and J. Reichel, *ibid.* **450**, 272 (2007).

[11] In contrast to many experiments (e.g., Refs. [18–20]), here the D_1 line is preferred to the D_2 line. The reason is that under the same detuning, the D_1 scheme yields the same coupling with the magnetization as the D_2 scheme, while the coupling with the density is only one half, so the disturbance introduced is smaller.

[12] K. L. Corwin, S. J. M. Kuppens, D. Cho, and C. E. Wieman, Phys. Rev. Lett. **83**, 1311 (1999).

[13] J. M. Higbie, L. E. Sadler, S. Inouye, A. P. Chikkatur, S. R. Leslie, K. L. Moore, V. Savalli, and D. M. Stamper-Kurn, Phys. Rev. Lett. **95**, 050401 (2005).

[14] Y. Liu, S. Jung, S. E. Maxwell, L. D. Turner, E. Tiesinga, and P. D. Lett, Phys. Rev. Lett. **102**, 125301 (2009); Y. Liu, E. Gomez, S. E. Maxwell, L. D. Turner, E. Tiesinga, and P. D. Lett, *ibid.* **102**, 225301 (2009).

[15] I. Carusotto and E. J. Mueller, J. Phys. B **37**, S115 (2004).

[16] J. M. Zhang, W. M. Liu, and D. L. Zhou, Phys. Rev. A **77**, 033620 (2008).

[17] J. Kronjäger, C. Becker, P. Navez, K. Bongs, and K. Sengstock, Phys. Rev. Lett. **97**, 110404 (2006).

[18] F. Brennecke, S. Ritter, T. Donner, and T. Esslinger, Science **322**, 235 (2008); S. Ritter, F. Brennecke, K. Baumann, T. Donner, C. Guerlin, and T. Esslinger, Appl. Phys. B: Lasers Opt. **95**, 213 (2009).

[19] S. Gupta, K. L. Moore, K. W. Murch, and D. M. Stamper-Kurn, Phys. Rev. Lett. **99**, 213601 (2007).

[20] J. A. Sauer, K. M. Fortier, M. S. Chang, C. D. Hamley, and M. S. Chapman, Phys. Rev. A **69**, 051804(R) (2004); K. M. Fortier, S. Y. Kim, M. J. Gibbons, P. Ahmadi, and M. S. Chapman, Phys. Rev. Lett. **98**, 233601 (2007).

[21] Experimentally the total atom number N cannot be determined precisely, so we cannot distinguish the AFM and FM ground states just by the shift of the spectra.

[22] J. M. Zhang, W. M. Liu, and D. L. Zhou, Phys. Rev. A **78**, 043618 (2008); J. M. Zhang, F. C. Cui, D. L. Zhou, and W. M. Liu, *ibid.* **79**, 033401 (2009).

[23] C. Cohen-Tannoudji and J. Dupont-Roc, Phys. Rev. A **5**, 968 (1972).

[24] I. H. Deutsch and P. S. Jessen, Phys. Rev. A **57**, 1972 (1998).

[25] D. Cho, J. Korean Phys. Soc. **30**, 373 (1997); J. M. Choi and D. Cho, J. Phys.: Conf. Ser. **80**, 012037 (2007).

[26] The condition that we do not resolve the hyperfine structure of the D_1 line allows us to take a common denominator.

[27] R. Grimm, M. Weidemüller, and Y. B. Ovchinnikov, Adv. At., Mol., Opt. Phys. **42**, 95 (2000).

[28] A. Daniel, Steck, "Rubidium 87 D Line Data," Revision 2.0.1, 2 May 2008, http://steck.us/alkalidata